Journal of Imaging Science and Technology® 55(5): 050606-1–050606-10, 2011.

Behavior of Ink Jet Printed Drops on a Corona-Treated Polymeric Film Substrate

Eleanor S. Betton, Wen-Kai Hsiao, Graham D. Martin▲, and Ian M. Hutchings▲
University of Cambridge, Institute for Manufacturing, Cambridge CB3 0FS, United Kingdom
E-mail: imh2@cam.ac.uk

Abstract. *The effects of corona discharge treatment (CDT) on ink drop impact and spreading on a coated polypropylene film substrate were investigated. Substrate surface energies were determined from static contact angles with water and ethylene glycol. The polar component increased with increasing CDT. Drops 39 μm in diameter of an acrylate-based UV-curable ink were printed on to the substrate, and the spreading process studied by high-speed photography. No changes occurred during the initial stages, but the wetting phase was shorter for higher doses of CDT. Drops spread further on substrates with low doses of CDT than with higher doses. White light interferometry was used to determine the final heights of drops after UV-curing. The height was significantly affected by CDT, with minimum height at low doses. The relationship was investigated between the static contact angle for large sessile drops and the equilibrium contact angle for printed drops after spreading. Contact angle measurements with millimeter-sized sessile drops of ink provide a reliable method to determine the effects of corona treatment on wetting by ink jet printed drops. © 2011 Society for Imaging Science and Technology.*
[DOI: 10.2352/J.ImagingSci.Technol.2011.55.5.050606]

INTRODUCTION

In recent years ink jet printing has become an increasingly flexible tool for manufacturing. Not only can traditional graphics be printed with extremely high quality, but now also at a much greater scale and speed than previously imagined. Other techniques using ink jet printheads are developing rapidly with good results across electronic, manufacturing, and biological engineering. Understanding the fundamentals of drop impact on to a solid surface is essential for controlling the shape and position of the deposited material. In a graphics context, this would determine the quality of an image, but in other applications it can influence whether a pixel in a display screen operates correctly—a living cell is in the right place—or if a circuit will conduct electricity.

Many applications require fluids to be deposited on to a poorly wetting surface, such as a polymer film, coated glass, or silicon. In order to achieve good adhesion the ink must wet the surface adequately. Substrates, therefore, often have their surfaces modified by corona discharge treatment (CDT), which increases their surface energy, and therefore enhances the wettability.

▲IS&T member.

Received Mar. 11, 2011; accepted for publication Jun. 8, 2011; published online Nov. 2, 2011
1062-3701/2011/55(5)050606/10/$20.00.

The various phenomena involved in liquid drop impact and spreading have been widely investigated for many different substrates and impact conditions. Four stages of impact have been defined by Rioboo et al.[1] as the kinematic, spreading, relaxation, and wetting phases. The timescale and rate of change of contact diameter in each phase together determine the final drop diameter. Several approaches to predicting this from the initial conditions have been made over the last 20 years with considerable success. However, there is little literature on the behavior of sub-millimeter drops, and currently none which examines the effects of CDT on drop impact and spreading behavior.

Corona treatment is used widely across the printing industry to increase the surface energy of polymeric films and metallic foils. The corona discharge is produced by electrodes connected to a high-voltage generator which ionizes the air between them and the surface of the film, which is backed by a grounded base roll. The ions produced are believed to oxidize the surface of the substrate, increasing its surface energy and thus reducing the contact angle between the printed fluid and the substrate (e.g., Kannangara et al.[2]).

Investigations by Meiron and Saguy[3] into the effect of corona treatment on high surface energy polymers showed that the increase in surface energy came from the polar component of free surface energy. This is supported by chemical analysis of corona-treated surfaces by Briggs et al.[4] who found a 3.5% increase in oxygen-based functional groups for a low level of corona treatment (final surface energy 44 mJ m^{-2}) and a 4.7% increase for a higher level of treatment (surface energy 59 mJ m^{-2}). Jones et al.[5] and O'Hare et al.[6] investigated the surface topography of corona-treated polypropylene, using atomic force microscopy (AFM) to image the surface before and after treatment. They suggested that the surface energy was affected by the formation of low molecular weight oxidized material.

The objective of the present work was to determine the effects of different doses of CDT, representative of commercial printing practice, on the spreading of ink drops on a typical industrial polypropylene-based film substrate. The change in surface energy was investigated, as well as its influence on the deposition behavior of 39 μm diameter droplets of a UV-curable ink impacting at 2.7 m/s, during both the kinematic and spreading phases. Methods of

calculating the maximum drop diameter, measured at the end of the spreading phase, were compared, and the dependence of final drop diameter on the level of CDT was studied for drops printed under conditions typical of industrial ink jet printing.

EXPERIMENTAL METHODS AND MATERIALS

The substrate used in these experiments was a top-coated biaxially orientated polypropylene-based film manufactured by UPM (UPM, Helsinki, Finland). Printing and drop impact experiments were performed with a commercial UV-curable acrylate-based graphics ink (UFX, SunJet, UK). Corona treatment was carried out with a commercial machine (CP-LAB, Vetaphone A/S, Denmark) in ambient air, and all printing experiments and measurements were carried out within 1 h of corona treatment. During corona treatment a sample of the polymer film was secured to the silicone-covered ground electrode roller with tape, while ensuring that there were no air bubbles between the film and the roller. The corona dose applied to the substrate was varied by controlling the speed of the roller, the power applied, and the treatment duration. Corona doses are stated below in units of $\mathrm{Wmin/m^2}$ ($100\ \mathrm{Wmin/m^2} = 6\ \mathrm{kJ/m^2} = 0.6\ \mathrm{J/cm^2}$).

Static contact angles were measured by the sessile drop method as described by Marmur,[7] with millimeter-sized drops of the UV-curable ink, triple-distilled water, and ethylene glycol. Ten measurements of contact angle were taken and averaged for each combination of fluid and surface, with a typical measurement error of $\pm 1.8^\circ$.

Deposition experiments were carried out with the same UV-curable ink in a modified version of the imaging rig described by Hsiao et al.[8] Figure 1 shows the optical setup used to image the impact and spreading of the ink drops. A piezoelectric drop-on-demand printhead (Xaar 126/80, Xaar plc, UK) was used to produce individual 38.5 μm $\pm$ 0.5 μm diameter drops traveling at 2.7 m/s $\pm$ 0.1 m/s. For this ink, these conditions correspond to a Reynolds number for jet formation of approximately 11.2 and a Weber number of approximately 8.9. Drop spreading was recorded for a period of about 300 ms after impact on to the film. This cut-off time was used because in industrial printing UV-curable inks are typically pinned within this timescale with a low dose of UV light to prevent further spreading.

The early stages (0–200 μs) of drop impact were captured with an ultra high speed video camera (Hypervision HPV-1, Shimadzu, Japan) coupled with a Navitar 12 $\times$ zoom lens system. Illumination for these experiments was provided by a high power xenon flash system (AD500, Specialised Imaging). The 1.5 ms duration 500 J flash was focused on to the impacting drop with a custom-made condenser to further intensify the illumination. Images were captured at 500,000 frames per second for 102 frames, with a resolution of 0.66 μm per pixel. The later stages (200 μs–285 ms) of drop spreading were studied with a high-speed video camera (Phantom V7.3) recording at 21,000

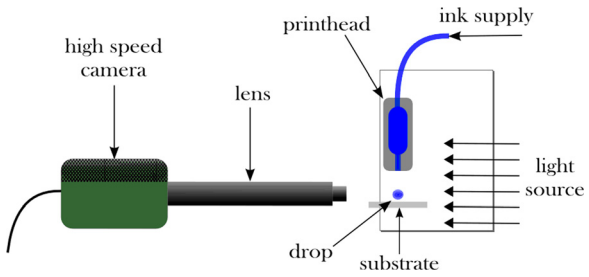

Figure 1. Experimental setup used to study drop impact and spreading for 39 μm drops travelling at 2.7 m/s. The types of cameras and light sources used to study the different stages of impact and spreading are described in the text.

frames per second. The difference in camera sensor size reduced the resolution in this case to 0.88 μm per pixel. In these experiments the drops were illuminated with a 150 W continuous halogen light source (Flexilux) via a light guide (Microtec), focused through a microscope objective to achieve a local high light intensity. Experiments showed that the heating effect of the continuous illumination was negligible, with a temperature rise of only 2 K after 1 h being detected with a thermocouple placed on the substrate at the drop impact position.

Image analysis was carried out with a MatLab program which used a gray threshold to convert the images to binary. The edges of the drop were detected, and the reflected image of the drop in the substrate was cropped below the baseline. The drop height and diameter were then measured. The contact angle was found by fitting a second order curve to the edge pixels and calculating the angle between its tangent and the baseline. Details of the image analysis methods can be found elsewhere.[9]

To study the effect of surface treatment on printed dot morphology in a typical industrial ink jet printing system, a commercial printer module with corona treating station was also used to print individual drops on to a moving web substrate. This system produced drops from a grayscale piezoelectric drop-on-demand printhead (Xaar 1001, Xaar plc, UK) which were cured within 100 ms of printing by passing under a 375 nm wavelength UV lamp. The drop volume prior to impact could be varied from 6 to 42 pl by using the grayscale function of the printhead. The final printed drop profile was measured with a white-light interferometer (Wyko NT3300), capable of measuring features between 0.1 nm and 2 mm in height. The heights and widths of the cured drops were measured in two orthogonal directions in the plane of the substrate, and measurements were repeated for a minimum of three drops for each sample.

Fourier transform infra-red spectroscopy (FTIR) measurements were made on the surfaces of polymer film samples with a Bruker Tensor 27 spectrometer operating in attenuated total reflection (ATR) mode. The samples were analyzed approximately 30 min after corona treatment, and measurements were repeated on several different regions on each sample.

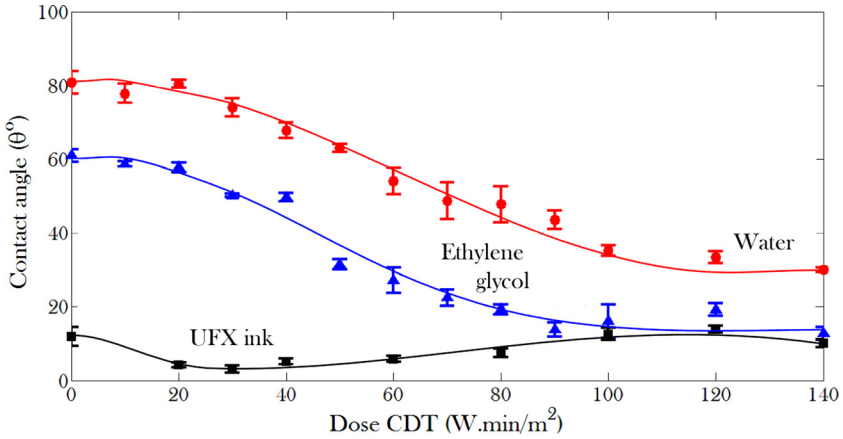

Figure 2. Measurements of static contact angle for millimeter-sized drops of water (circles), ethylene glycol (triangles), and UV-curable ink (squares) on substrates with different levels of CDT.

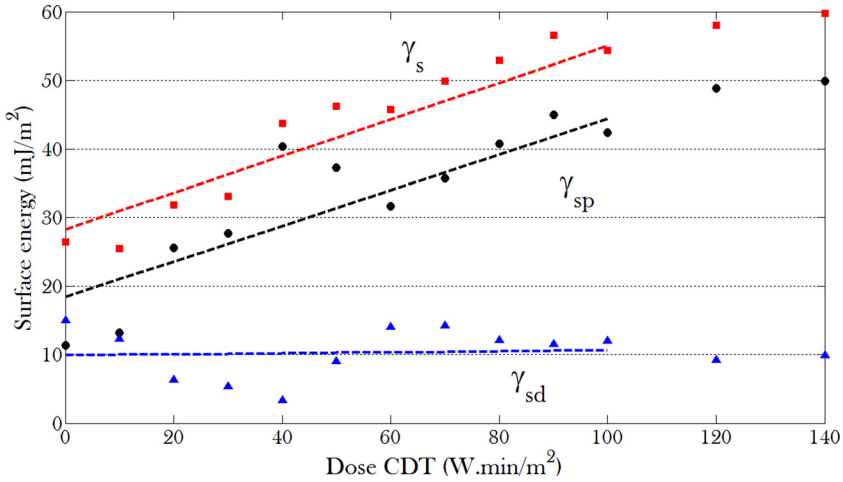

Figure 3. Surface energy calculated by the Owens and Wendt equation (1) from contact angles measured with water and ethylene glycol: polar component (circles), dispersive component (triangles), and total surface energy (squares) for substrates with different levels of CDT.

RESULTS AND DISCUSSION

Static Wetting Behavior

Contact angle analysis is widely used for estimating the surface energy of a substrate. The contact angle values determined for millimeter-sized drops of water, ethylene glycol, and UV ink on the polymer substrate after corona treatment to levels between 0 and 140 Wmin/m^2 are plotted in Figure 2. It is clear that increasing the level of CDT decreased the contact angle for both water and ethylene glycol. However, for the UV ink the contact angle decreased slightly for low levels of CDT and then increased at higher levels, above about 30 Wmin/m^2. The static contact angle formed on the substrate with all three fluids levels off at doses above 100 Wmin/m^2. Similar behaviour was reported by Jones et al.[5] and O'Hare et al.[6] and is probably associated with saturation of the chemical changes induced in the uppermost surface regions of the coated film by the corona treatment.

The total surface energy of the substrate (γ_s) and its polar (γ_{sp}) and dispersive (γ_{sd}) components were calculated by using the Owens and Wendt equation[10] using known values for the liquid's dispersive component (γ_{ld}) and polar component (γ_{lp})

$$(1+\cos\theta)\gamma_l = 2\sqrt{\gamma_{sd}\gamma_{ld}} + 2\sqrt{\gamma_{sp}\gamma_{lp}} \qquad (1)$$

where $\gamma_l = \gamma_{ld} + \gamma_{lp}$ is the free surface energy of the liquid and θ is the static contact angle for the liquid on the substrate. The dispersive component represents the contribution of van der Waals forces to the free surface energy, while the polar component represents the contribution to the free surface energy caused by polar bonds. By plotting the contact angles measured with water and ethylene glycol, we found the polar and dispersive component of free surface energy of the surface using linear regression, with the results shown in Figure 3. The total free surface energy increased with increasing treatment level due almost exclusively to an increase in the polar component: there was little change in the dispersive component. This observation is consistent with a higher level of CDT being associated with a higher level of surface oxidation, leading to an increase in

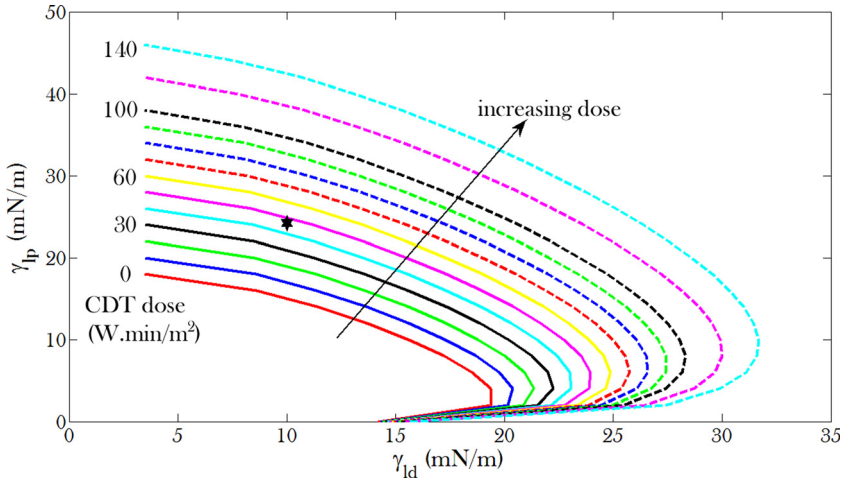

Figure 4. Wetting envelopes derived from static measurements of contact angle for different levels of corona treatment from 0 to 140 Wmin/m^2. The star shows the values for the UV-curable ink.

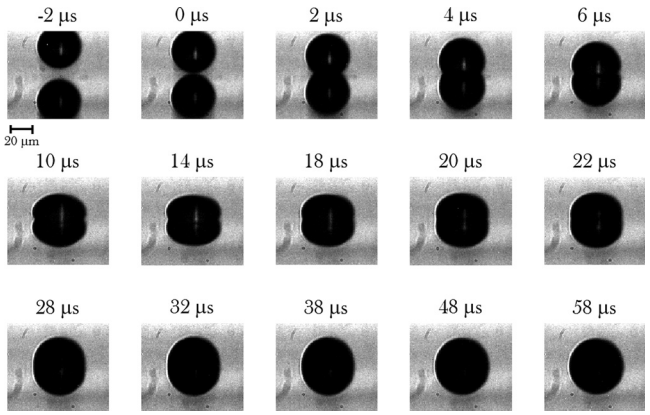

Figure 5. Images showing dynamic drop spreading during the impact of a 39 μm drop of UV-curable ink at 2.7 m/s on a polymer film after corona treatment at 100 Wmin/m^2. The horizontal center-line of each frame represents the surface of the substrate, and the image of the drop is reflected in this line in each case.

the polar component. In their studies of corona treatment of uncoated polypropylene, O'Hare et al.[6] also found little change in the dispersive component with the level of CDT. However, they reported that the polar component for their untreated film was zero; the presence of a significant polar component in Fig. 3, even in the untreated condition, is associated with the presence of a polar coating on this film.

The contact angles measured with the two test fluids, water and ethylene glycol, were also used to compute wetting envelopes for the different levels of corona treatment. The contours corresponding to a 0° contact angle (i.e., full wetting) for each level of CDT are shown in Figure 4. This can in principle be used to predict how increasing the level of CDT should increase the wettability of the substrate. The point corresponding to the UV-curable ink lies between the contours corresponding to doses of 40 and 50 Wmin/m^2, which suggests that this film would require a level of corona treatment beyond 40 Wmin/m^2 for the ink to wet it completely.

This prediction is not, however, fully consistent with the measured values of contact angle for the ink, which show the greatest wettability for doses between 20 and 40 Wmin/m^2, with still higher doses of CDT causing a decrease in wettability. This illustrates that although such wetting envelopes may be useful for estimating changes in surface energy, they are less accurate for estimating the wetting properties of specific inks because they cannot reflect the more complex interactions between inks and substrates. As discussed by Lee et al.[11] and Chhatre et al.,[12] accurate prediction of the contact angle depends on a more detailed consideration of the chemical nature of both the fluid and the substrate, which cannot be fully described by values of polar and dispersive energies.

Dynamic Analysis

In order to study the effects of corona treatment on the deposition of drops under practical printing conditions (i.e., with very small drops being deposited dynamically), the spreading behavior of printed drops of the UV-curable ink was imaged continuously during the kinematic, spreading, and relaxation phases. In all these dynamic experiments the drops had an initial diameter D_o of 39 μm and a velocity at impact, U_o of 2.7 m/s. The drop diameters were then analyzed in terms of spread factor and non-dimensional time. The non-dimensional time, t^*, is defined by $t^* = t\ U_o/D_o$. The spread factor, β, is the instantaneous diameter of the drop, D, divided by the initial diameter of the drop, $\beta = D/D_o$. In order to examine the effects of CDT on the kinematic phase of impact the first few hundred microseconds were also imaged as described above. An example of a sequence of images is shown in Figure 5.

The non-dimensional drop height during the first 100 μs of impact, defined as $h/r_o = 2h/D_o$ where h is the instantaneous drop height, is plotted in Figure 6 with the different phases of spreading marked. The difference between the

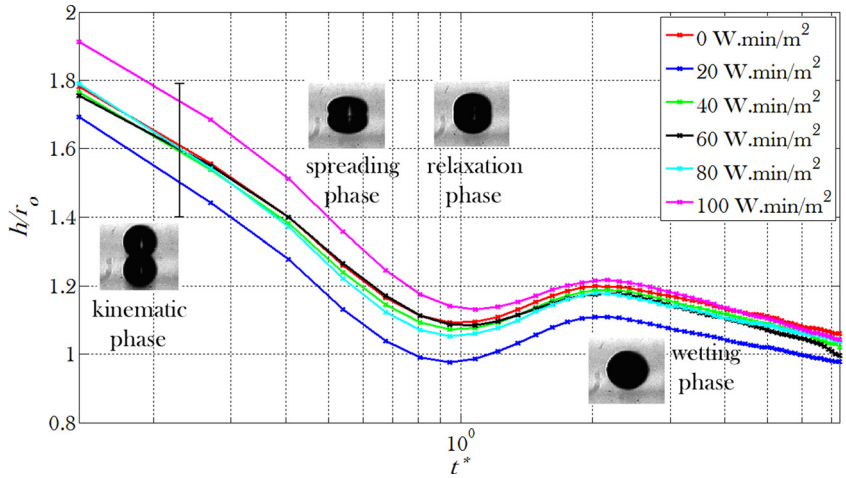

Figure 6. Non-dimensional drop height h/r_o plotted against non-dimensional time t^* for impact of 39 μm diameter drops of UV-curable ink at 2.7 m/s on polymer substrates with different doses of CDT during the impact stage of spreading. The different phases of spreading are marked. The error bar shows the typical variations associated with the measured drop height (± 2 μm).

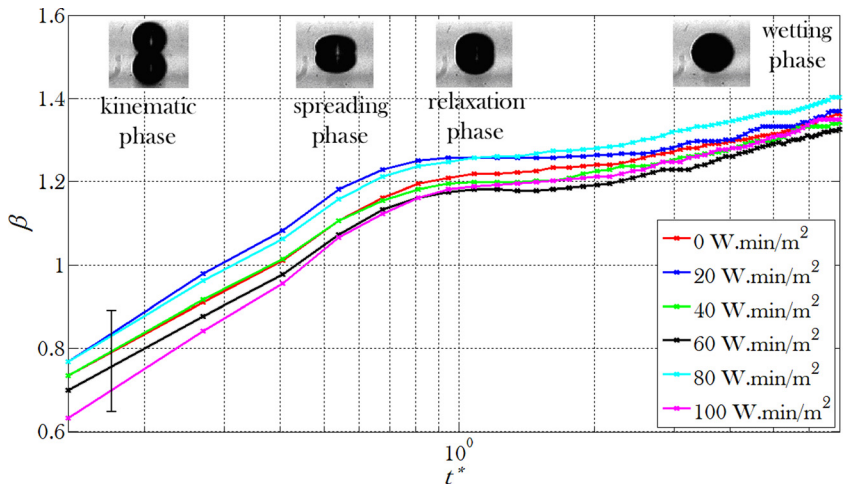

Figure 7. Spread factor plotted against non-dimensional time t^* for impact of 39 μm drops of UV ink at 2.7 m/s on polymer substrates with different doses of CDT during the earliest stages of spreading. The different phases of spreading are marked. The error bar shows the typical uncertainty associated with the measured drop diameter (± 2 μm).

results for the different levels of CDT is a maximum of ± 2 μm. This is within the range of random errors, either due to timing errors involved in the drop impact or variation in lighting affecting the image analysis by causing small variations in the gray level thresholding process. This suggests that the spreading behaviour remains effectively unchanged during the impact stage for substrates treated with levels of corona treatment between 20 and 100 Wmin/m^2.

During the kinematic phase, the drop height h decreases as the drop impacts the surface and the fluid is predominantly moving vertically. The spreading phase begins as the fluid begins to move horizontally, forming a flattened disc shape. The maximum spreading diameter occurs when the drop height is at a minimum. Beyond this point the drop height increases as the drop relaxes. The surface energy of the drop drives it to form a spherical cap, which is the lowest energy shape for the drop (under these conditions where gravitational forces are negligibly small). During its relaxation from a flattened disc shape to a spherical cap, the contact line remains pinned. The wetting phase begins after this as the contact line then begins to move outwards and the fluid progressively wets the substrate.

The spreading diameter during the impact stages, including the early wetting phase, is plotted in Figure 7 for impact on the polymer film with a range of doses of CDT. Different levels of CDT do not significantly change the deposit diameter or the duration of the kinematic phase. Similarly, the spreading, relaxation, and early wetting phases (for $t^* < 10$) remain unchanged by the different levels of CDT. This is not unexpected as the earliest impact stages are controlled by inertia and the effects of substrate surface

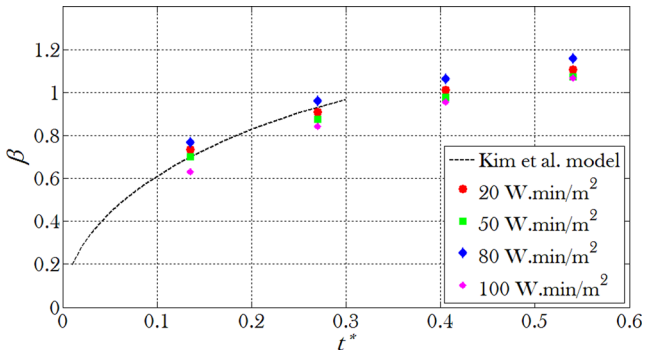

Figure 8. Spread factor during the kinematic phase of impact for drops spreading on polymer films corona-treated with doses between 20 and 100 Wmin/m^2. The dashed line is the prediction from the model of Kim et al.[13]

energy have not yet come into play. The kinematic stage of spreading has been investigated by Kim et al.[13] who developed a model in which the volume displaced by the substrate as the drop descends is transferred to the edges of the drop. A simplified model was developed by Rioboo et al.[1] which does not account for the displaced fluid. Both models show good agreement with the experimental data for drops spreading on substrates treated with all doses of CDT during the kinematic phase, as shown in Figure 8.

The maximum spread diameter, D_{max}, and associated maximum spread factor, $\beta_{max} = D_{max}/D_o$, were measured at the end of the spreading phase for ink drops printed on substrates after different levels of CDT. The values are plotted in Figure 9 against the static contact angle measured for millimeter-sized drops of the same ink on the substrate. Many methods have been proposed for predicting β_{max}. The models of Asai et al.[14] and Scheller and Bousfield[15] are based on the Weber and Reynolds numbers and do not require a contact angle measurement. Both are empirical, with the model of Asai et al. being based on data for the sub-millimeter drops representative of ink jet printing. The model of Chandra and Avesidian[16] is based on energy conservation with an assumption of a cylindrical drop shape at β_{max}. Fukai et al.[17] developed a semi-empirical model based on Chandra and Avesidian's work. For an alternative model, a spherical cap shape can be assumed based on volume conservation calculated from the static contact angle.

The predictions from each of these models are also plotted in Fig. 9. The model of Asai et al.[14] gives the best agreement with the experimental results. The model based on a spherical cap and the value of quasi-static contact angle overestimates the final diameter. Use of the advancing contact angle together with volume conservation also overestimates β_{max}. Our results suggest that existing energy-based analytical models are insufficiently accurate in predicting drop deposition behaviour under conditions typical of ink jet printing. A simple empirical model specific to the relevant Weber and Reynolds number is shown to produce better prediction of β_{max}.

Images of the wetting stage of drop spreading were captured at 21,000 fps. Figure 10 shows examples from a sequence captured over the first 240 ms, for drops impacting on polymer films treated to levels of 20 and 100 Wmin/m^2. It is clear from these images that the drop deposited on the substrate treated with 20 Wmin/m^2 spreads to a greater extent than the drop deposited on the substrate treated with the higher dose.

The difference in spreading behavior over long time scales (up to $t^* > 10^4$) for different intensities of CDT becomes evident in Figure 11 which shows the spread factor plotted against non-dimensional time. Unlike in the earlier stages of impact, a change is now observed in the wetting and equilibrium stages. The main difference is in the time taken for the fluid to reach equilibrium. For substrates treated with low doses of CDT the wetting phase continued for longer, with substrates treated to 0–40 Wmin/m^2 not reaching equilibrium within the 285 ms timescale ($t^* = 2 \times 10^4$). Substrates which had been corona treated above 80 Wmin/m^2 showed a much shorter wetting phase, with the spread factor leveling off as early as 29 ms ($t^* = 2 \times 10^3$). The behavior for the substrate treated with 60 Wmin/m^2 lies between the two, reaching equilibrium at approx 60 ms after impact ($t^* = 4 \times 10^3$).

During the extended wetting phase the contact angle follows the same trends as those seen for the spread factor and normalized height. Figure 12 shows the contact angle measured during the first 285 ms after impact. The initial stages show a rapid decrease with time. The contact angle then continues to decrease during the wetting phase until it approaches the equilibrium contact angle. The drops on the untreated substrate and on substrates with the two lowest doses of corona treatment do not reach equilibrium within 285 ms, whereas for those with a higher treatment level the contact angle eventually becomes constant at approximately 15°.

Figure 13 compares the equilibrium contact angles, measured 285 ms after drop impact, with the static contact angle as plotted in Fig. 2, measured for millimeter-sized sessile drops. For substrates with corona treatment of >40 Wmin/m^2 the static contact angles for the ink shown in Fig. 2 were on average 5° lower than the equilibrium contact angle measured after spreading of a printed drop. A similar result was found by Son et al.,[18] who found that the static and equilibrium contact angles differed, with the equilibrium contact angle after drop impact being greater than the static contact angle for substrates with a low contact angle. They suggested that this is due to energy being dissipated at the contact line leading to pinning of the contact line before the static contact angle is reached. For surfaces treated with doses of CDT between 10 and 40 Wmin/m^2 the contact angle measured after 285 ms of spreading was higher than that on the untreated substrate, because the drop was still wetting the substrate at that point and had not yet reached equilibrium.

Printed Drop Size

For comparison with the experimental results obtained with individual drops in laboratory experiments, printed

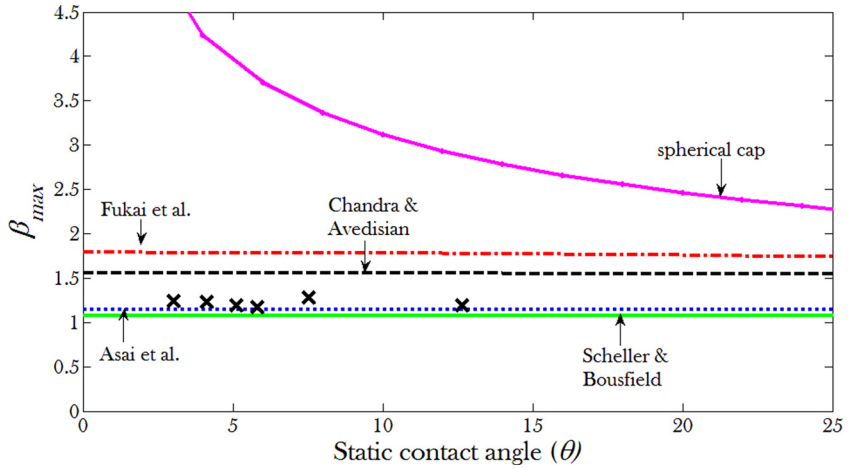

Figure 9. Maximum spread factor for drops of UV-curable ink printed on the polymer substrate with different doses of CDT. Maximum spread factor, β_{max}, is plotted against the static contact angle for the ink on the same substrates (crosses).

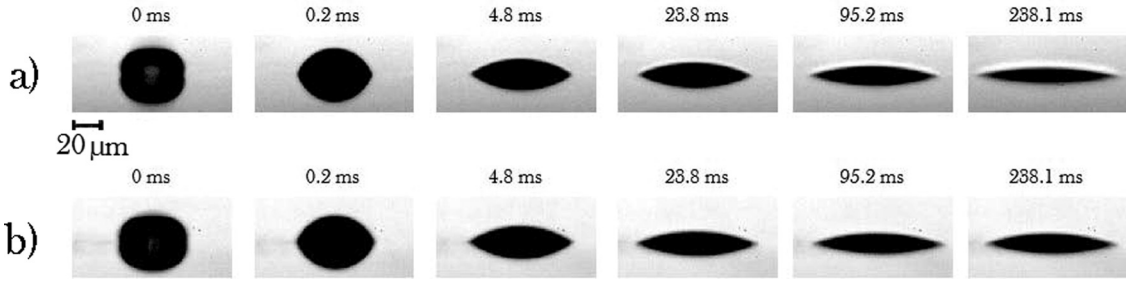

Figure 10. Images captured at 21,000 fps for a 39 μm UFX ink drop impacting on a polymer substrate after corona-treatment with doses of (a) 20 Wmin/m^2 and (b) 100 Wmin/m^2.

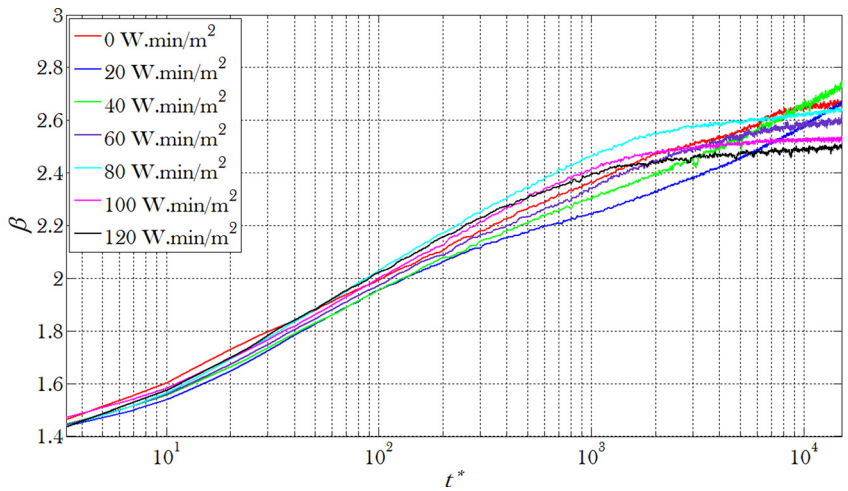

Figure 11. Spread factor plotted against non-dimensional time t^* for impact of 39 μm drops of UV ink at 2.7 m/s on polymer substrates with different doses of CDT during the wetting stages of spreading.

samples generated under typical deposition conditions in a full-scale industrial web printing system were also analyzed. Droplets of the same UV-curable ink were printed from a Xaar 1001 head on to the same polymer substrate which had been corona treated (with a commercial in-line system) and were UV-cured ~100 ms after printing. White-light interferometry was then used to measure the final height of the solidified drops. The sizes of the drops were varied by increasing the gray-scale level generated from the print-head, from 1 to 6 drops per dot (dpd). For this particular

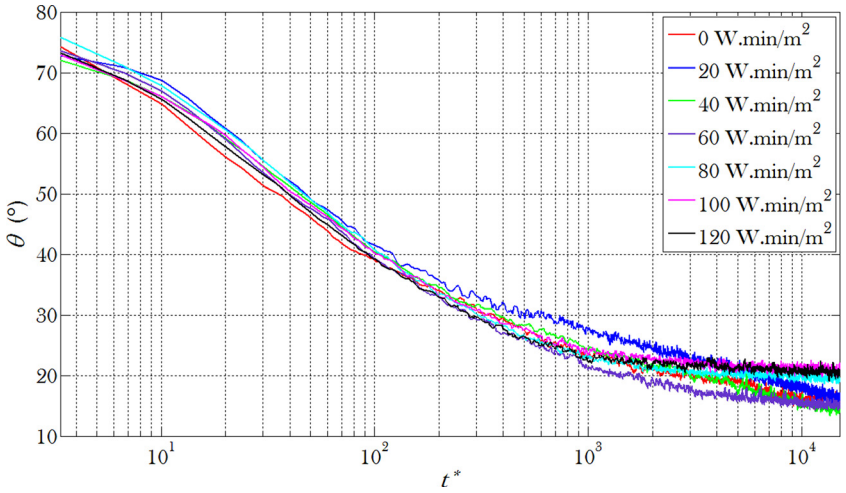

Figure 12. Measured contact angle, θ, plotted against non-dimensional time t^* for impact of 39 μm drops of UV ink at 2.7 m/s on polymer substrates with different doses of CDT during the wetting stages of spreading.

printhead, each step in the gray-scale level corresponds to a change of 6 pl in total drop volume.

The drop heights measured by white light interferometry for printed and cured drops on polymer substrates treated with different doses of CDT are shown in Figure 14. The drop diameter could not be measured accurately with this technique due to the low contact angle of the drop. The minimum drop height occurs for all drop sizes on substrates treated with a dose between 20 and 40 Wmin/m^2 of corona. This supports the results from the spreading experiments, which found that the largest diameter drops were formed on substrates with corona doses lying between 20 and 40 Wmin/m^2. This suggests that the drop diameter, measured towards the end of the wetting phase of drop spreading, can be used to estimate the optimum corona treatment to be used in an industrial printing system.

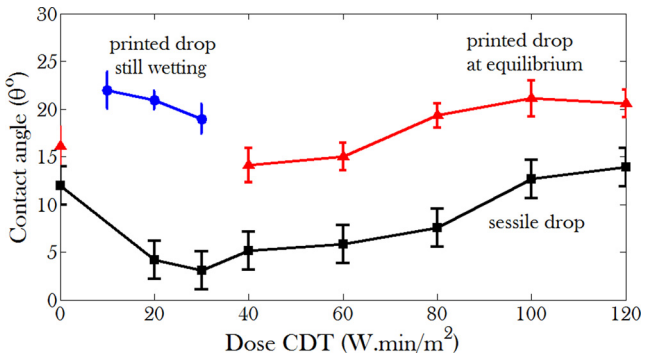

Figure 13. Equilibrium contact angle (triangles) measured for drops 285 ms after drop impact compared with the static contact angle (squares) measured for millimeter-sized sessile drops placed on a surface (see Fig. 2), for different doses of CDT. For corona treatments between 10 and 30 Wmin/m^2 the drops had still not reached equilibrium after 285 ms and were still extending over the surface.

FTIR Analysis

To investigate possible chemical changes on the substrate surface induced by corona discharge treatment, Fourier transform infrared spectroscopy (FTIR) in attenuated total reflection mode was used to analyse the film samples before and after CDT at a range of doses. The results for measurements on untreated film and for samples treated with doses from 40 to 120 Wmin/m^2 are shown in Figure 15. It is clear that there is no detectable difference between the spectra from the untreated and treated films. Furthermore, the strong peak at a wavenumber of 1735 cm^{-1} which is associated with carbonyl C=O bonds is present for all the samples although it would be absent for untreated, uncoated polypropylene. Guimond et al.[19] studied the corona treatment of uncoated polypropylene films and showed that the C=O absorption peak, absent in their untreated material, became strong after CDT. It is probable that the strong C=O absorption peak in the present coated film is due to the coating material and that any further oxidation caused by CDT, which may affect only a thin surface layer, has a negligible effect on the measured IR spectrum. The signal from FTIR spectroscopy in ATR mode relates to a depth of ~1 μm for this wavenumber in polypropylene, whereas the contact angle measurements (and hence the spreading of a printed drop) are influenced by the material properties to a much shallower depth: perhaps the outermost 0.5 nm.[20] In the present work it is unlikely that any significant chemical effects induced by the CDT will have been reversed in the short interval (~30 min) between treatment and analysis, as the static contact angles for the ink and the other fluids remained essentially the same for several hours after treatment.

DISCUSSION

This study investigated in detail the effect of corona discharge treatment on parameters relevant to ink drop deposition on a typical commercial polypropylene-based film under industrial ink jet web printing conditions. While an improvement in wetting for the UV-curing ink on the polymer film was found after low levels of CDT treatment (20

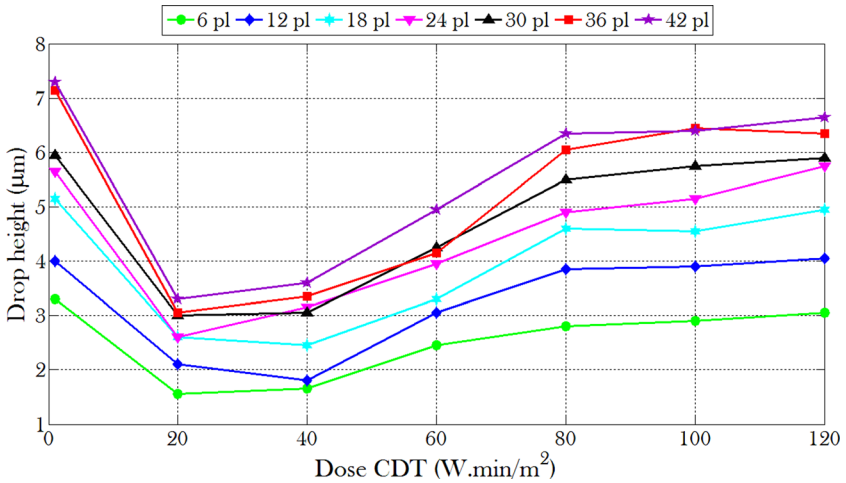

Figure 14. Final height measured by white-light interferometry for printed and cured dots on polymer substrates with different doses of corona treatment, for six different drop sizes (gray-scale levels).

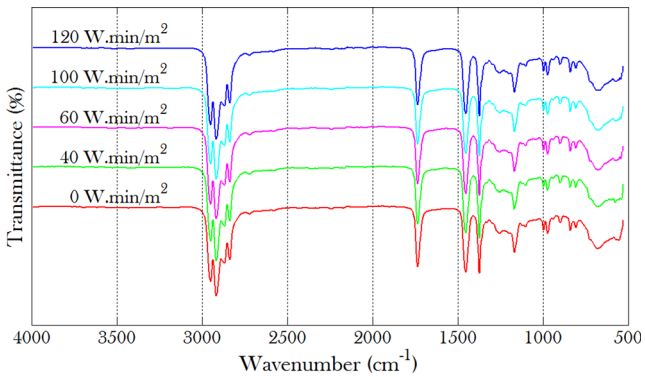

Figure 15. FTIR-ATR spectra of polymer surfaces after treatment with different doses of CDT. The traces are offset vertically for ease of comparison.

and 40 Wmin/m^2), further treatment was found to be detrimental to wetting. This observation appears inconsistent with the trends in static contact angle observed with millimeter-sized drops of water and ethylene glycol. For these liquids, surface wetting improved continuously with increasing levels of CDT. Similarly, a disagreement was found when using wetting envelope analysis to predict the CDT threshold for maximum ink-film wetting. The minimum dose of corona treatment required for complete ink wetting suggested by the wetting envelopes (40 Wmin/m^2) was found to coincide with the level of CDT above which the static contact angle of the ink began to increase. These observations suggest that for this system of a typical UV-curable ink on a coated polypropylene film, increasing the CDT level does not necessarily improve wetting and also that it is unsafe to draw conclusions about wetting by an acrylate ink from contact angle measurements made with test fluids such as water and ethylene glycol which have quite different chemical properties. However, contact angle measurements with millimeter-sized sessile drops of the same ink do provide a reliable method to determine the effects of corona treatment on wetting by ink jet printed drops.

The effect on wetting of an increase of CDT level beyond 40 Wmin/m^2 was also evident during the dynamics of ink drop deposition. Analysis of the high-speed image data suggests that the effect of increasing the level of CDT on drop spreading is minimal during the inertia-dominated kinematic and spreading phases. However, the improvement in wetting caused by increasing the level of CDT from 20 to 60 Wmin/m^2 led to a prolonged wetting phase. Further increases in CDT decreased the wetting phase duration, with the drop reaching equilibrium in a shorter time and achieving a smaller final diameter.

A crucial parameter that characterizes the drop deposition dynamics is the maximum spreading diameter or, in non-dimensional form, the maximum spread factor, β. Several approaches to predicting the maximum spread factor have been compared with our experimental measurements. The semi-empirical model based on specific Weber and Reynolds numbers, as proposed by Asai et al.,[14] gave the most accurate prediction for this experimental setup. It was also clear that the analytical approach of estimating the maximum spread factor based on energy conservation and various interpretations of contact angle is insufficient to predict the dynamics of deposition behavior for the small ink drops used in printing. The discrepancy is likely to be caused by the fact that the impact and spreading of a smaller ink drop on a surface are more prone to contact line pinning induced by surface irregularities.

The effect of surface treatment on printed dot morphology was studied with white light interferometry. The influence of surface modification by CDT was evident and became more pronounced for larger drop volumes. The height of the dot profile decreased initially for low doses of CDT (0–20 Wmin/m^2) and then gradually increased with increasing dose of CDT (20–120 Wmin/m^2). This trend is consistent with the relationship observed between CDT and the resultant static contact angles measured with millimeter-sized sessile drops (with greater contact angle leading to greater dot height). This corresponds well with

the equilibrium contact angle measurements taken at the end of the wetting phase after impact for substrates treated with doses above 40 Wmin/m^2. The observation therefore confirms that the spreading diameter seen in dynamic experiments can be used to predict the effect of corona discharge treatment on final print quality under industrial ink jet printing conditions.

CONCLUSIONS

Increasing the dose of CDT on a commercial, coated biaxially oriented polypropylene film increased the polar component of its free surface energy. This caused a consistent decrease in static contact angle, measured with millimeter-sized drops of water and ethylene glycol, but not for UV-curable ink for which the behavior was more complex. CDT was found not to affect the early impact stages of spreading for small ink drops deposited from a drop-on-demand ink jet printhead. High doses of CDT caused a decrease in the duration of the wetting stage. This caused a decrease in drop diameter measured at later stages of drop spreading for drops printed on to the substrate with higher doses of CDT. These results were supported by an increase in drop height measured by white-light interferometry for drops printed in an industrial system on substrates treated with doses of CDT greater than 40 Wmin/m^2. The equilibrium contact angle, measured after the drop had impacted and spread, was consistently larger than the static contact angle measured for millimeter-sized sessile drops.

It is suggested that it is unsafe to draw conclusions about wetting by an acrylate ink from contact angle measurements made with test fluids such as water and ethylene glycol which have quite different chemical properties. However, contact angle measurements with millimeter-sized sessile drops of the same ink do provide a reliable method to determine the effects of corona treatment on wetting by ink jet printed drops.

ACKNOWLEDGEMENTS

This work was supported by FFEI Ltd and the Engineering and Physical Sciences Research Council (UK). The authors would also like to thank the EPSRC Engineering Instrument Pool for the loan of the Shimadzu ultra high speed camera system.

REFERENCES

[1] R. Rioboo, M. Marengo, and C. Tropea, Exp. Fluids, **33**, 112–124 (2002).
[2] D. Kannangara, H. Zhang, and W. Shen, Colloids Surf. A, **280**, 203–215 (2006).
[3] T. S. Meiron and I. S. Saguy, Food Res. Int. **40**(5), 653–659 (2007).
[4] D. Briggs, D. M. Brewis, R. H. Dahm, and I. W. Fletcher, Surf. Interface Anal., **35**, 156–167 (2003).
[5] V. Jones, M. Strobel, and M. J. Prokosch, Plasma Processes Polym., **2**, 547–553 (2005).
[6] L.-A. O'Hare, S. Leadley, and B. Parbhoo, Surf. Interface Anal., **33**, 335–342 (2002).
[7] A. Marmur, Soft Matter, **2**, 12–17 (2006).
[8] W.-K. Hsiao, S. D. Hoath, G. D. Martin, and I. M. Hutchings, J. Imaging Sci. Technol., **53**(5), 050304-(8) (2009).
[9] E. S. Betton, Ph.D. thesis, University of Cambridge, Cambridge, UK, 2011.
[10] D. K. Owens and R. C. Wendt, J. Appl. Polym. Sci., **13**(8), 1741–1747 (1969).
[11] S. Lee, J.-S. Park, and T. R. Lee, Langmuir, **24**, 4817–4826 (2008).
[12] S. S. Chhatre, J. O. Guardado, B. M. Moore, T. S. Haddad, J. M. Mabry, G. H. McKinley, and R. E. Cohen, Appl. Mater.Interfaces **2**(12), 3544–3554 (2010).
[13] H.-Y. Kim, Z. C. Feng, and J.-H. Chun, Phys.Fluids **12**(3), 531–541 (2000).
[14] A. Asai, M. Shioya, S. Hirasawa, and T. Okazaki, J. Imaging Sci. Technol., **37**, 205–207 (1993).
[15] B. L. Scheller and D. W. Bousfield, AIChE J., **41**, 1357–1367 (1995).
[16] S. Chandra and C. T. Avedisian, Proc. R. Soc. London Ser.A, **432**, 13–41 (1991).
[17] J. Fukai, M. Tanaka, and O. Miyatake, J. Chem. Eng. Jpn., **31**, 456–461 (1998).
[18] Y. Son, C. Kim, D. H. Yang, and D. J. Ahn, Langmuir, **24**, 2900–2907 (2007).
[19] S. Guimond, I. Radu, G. Czeremuszkin, D. J. Carlsson, and M.R. Wertheimer, Plasmas and Polym. **7**(1), 71–88 (2002).
[20] M. Strobel, M. J. Walzak, J. M. Hill, A. Lin, E. Karbashewski, and C. S. Lyons, J. Adhesion Sci. Technol. **9**(3), 365–383 (1995).